The rheology and processing of "edge sheared" colloidal polymer opals

Hon Sum Wong, Malcolm Mackley,[a] and Simon Butler

Department of Chemical Engineering and Biotechnology,
University of Cambridge, Cambridge CB2 3RA, United Kingdom

Jeremy Baumberg, David Snoswell,[b] Chris Finlayson,[c] and Qibin Zhao

Cavendish Laboratory, NanoPhotonics Centre,
University of Cambridge, Cambridge CB3 OHE, United Kingdom

Synopsis

This paper is concerned with the rheology and processing of solvent-free core shell "polymer opals" that consist of a soft outer shell grafted to hard colloidal polymer core particles. Strong iridescent colors can be produced by shearing the material in a certain way that causes the initially disordered spheres to rearrange into ordered crystalline structures and produce colors by diffraction and interference of multiple light scattering, similar to gemstone opals. The basic linear viscoelastic rheology of a polymer opal sample was determined as a function of temperature, and the material was found to be highly viscoelastic at all tested temperatures. A Cambridge multipass rheometer was specifically modified in order to make controlled mechanical measurements of initially disordered polymer opal tapes that were sandwiched between protective polyethylene terephthalate sheets. Axial extension, simple shear, and a novel "edge shearing" geometry were all evaluated, and multiple successive experiments of the edge shearing test were carried out at different temperatures. The optical development of colloidal ordering, measured as optical opalescence, was quantified by spectroscopy using visible backscattered light. The development of opalescence was found to be sensitive to the geometry of deformation and a number of process variables suggesting a complex interaction of parameters that caused the opalescence. In order to identify aspects of the deformation mechanism of the edge shearing experiment, a separate series of *in situ* optical experiments were carried out and this helped indicate the extent of simple shear generated with each edge shear deformation. The results show that strong ordering can be induced by successive edge shearing deformation. The results are relevant to polymer opal rheology, processing, and mechanisms relating to ordering within complex viscoelastic fluids. © *2014 The Society of Rheology*. [http://dx.doi.org/10.1122/1.4862920]

[a]Author to whom correspondence should be addressed; electronic mail: mrm5@cam.ac.uk
[b]Current address: Sclumberger Gould Research, Cambridge CB3 0EL, United Kingdom.
[c]Current address: Institute of Mathematics, Physics and Computer Science (IMPACS), Prifysgol Aberystwyth University, SY23 3BZ Wales, United Kingdom.

I. INTRODUCTION

Polymer opals are a relatively new and exciting class of materials that have unusual rheology, processing, and optical properties [see, for example, Pursiainen *et al.* (2005); Snoswell *et al.* (2010); Finlayson and Baumberg (2013)]. Following the development of monodisperse colloidal polymer particle suspensions in the 1950s [Alfrey *et al.* (1954)], it became clear that they could have interesting optical properties if ordered [see, for example, Hachisu *et al.* (1973)]. Subsequently, solvent-free polymer particle spheres have been developed of the type shown schematically in Fig. 1, where polymer chains are grafted to the outside of the particles in a manner that creates a solvent-free concentrated dispersion of monodisperse spheres within a highly viscoelastic matrix [see, for example, Ruhl *et al.* (2003); Viel *et al.* (2007)]. Because the spheres were of a diameter similar to the wavelength of light there is potential for these solvent-free materials to exhibit interesting photonic optical effects, particularly if the colloidal particles become ordered [see, for example, Ruhl *et al.* (2004); Pursiainen *et al.* (2007)].

A breakthrough was achieved with the development of an edge-induced rotational shearing (EIRS) process [Finlayson *et al.* (2011b)] shown schematically in Fig. 2. Repeated shearing at elevated temperature around a sharp edge can produce samples with improved reproducibly and uniformity of bulk-ordering, greatly enhancing both the intensity and chromaticity of the observed structural color. The application of shear ordering techniques to these solvent-free systems allow formation of permanent, mechanically robust composites in the solid-state. An attractive feature of elastomeric polymer opals is the tunability of their perceived color by the bending or stretch modification of the (111) plane spacing. As such, these "polymer opals" present opportunities for a step-change away from the monolithic architectures which are currently relied upon in the field of photonic structures and are a promising platform for next generation bulk-scale photonics materials, coatings, fibers, and sensors [Sussman *et al.* (2009); Finlayson *et al.* (2011a); Finlayson and Baumberg (2013)].

The effect of shear on the ordering and rheology of colloidal suspensions in a low viscosity matrix has been reported before, and in general, it has been found that simple shear is capable of creating order in concentrated colloidal systems [see, for example, Ackerson and Pusey (1988); Chen *et al.* (1992); Liu *et al.* (1993)] with an associated rheological general trend of shear thinning [Mewis *et al.* (1989)]. A number of authors [see, for example, Ackerson (1990); Haw *et al.* (1998); Koumakis *et al.* (2008); McMullan and Wagner (2009)] have reported the ordering of colloidal suspensions using oscillatory shear and a review on low viscosity base fluid ordering in steady and oscillatory simple shear is given by Vermant and Solomon (2005). As the concentration of suspension increases, complications such as jamming [see, for example, Trappe *et al.* (2001); Liu and Nagel (2010);
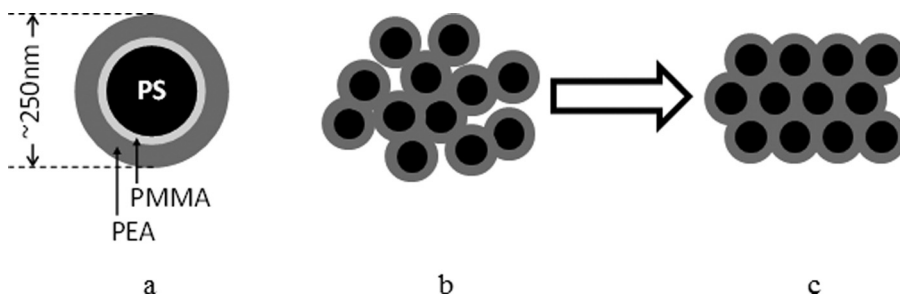
FIG. 1. Schematic diagram of polymer opal microstructure. (a) Core interlayer shell structure (b) and (c) Ordering of particles from disordered state to opalescent ordered state (Cambridge NanoPhotonic Centre, 2009).
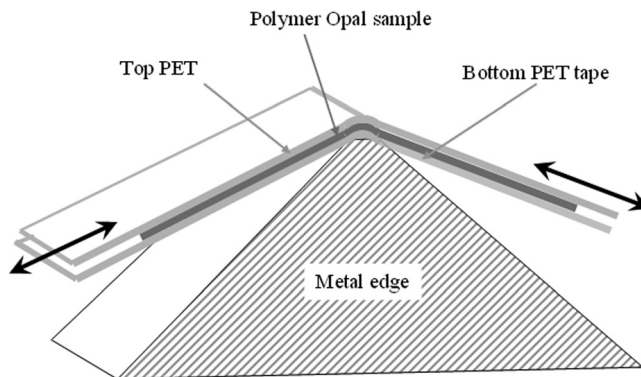
FIG. 2. Schematic diagram of the edge shearing process showing geometry of opal film sandwiched between PET films.

Kramb and Zukoskia (2011)] and high shear disorder [Catherall *et al*. (2000)] can also occur which makes generalization of microstructural behavior difficult.

The melt rheology and theory of commercial processable polymer melts is well documented and now understood [see, for example, Dealy and Wang (2013)]; however, as polymer melts become more intractable and rubberlike, both their rheology and process behavior become more difficult to characterize and understand [see, for example, White and Kim (2008)].

In this paper, a polymer opal sample is considered where the rheology is in a transition region between that of a polymer melt and a rubber. The material is difficult to process at all available temperatures, and depending on process history, the material may be ordered or not. The ability to directly visualize the ordering and hence shear history in the polymer opals through color changes aids understanding of flow induced ordering mechanisms and may give insight into the rheological behavior of the material. In addition to reporting temperature dependent rheological measurements of a polymer opal sample, this paper builds on the discovery by Finlayson *et al*. (2011b) that showed successive hand edge shearing can induce ordering of an initially disordered sample. A new way of carrying out machine controlled experiments has been developed by modifying a Cambridge multipass rheometer (MPR) [Mackley *et al*. (1995)] in order that systematic deformation experiments could be carried out as a function of a number of different variables that influence ordering. The test materials were then subsequently evaluated for their optical spectra response thereby enabling optimum process conditions for opalescence to be established.

II. OPAL MATERIAL

The polymeric opal material described in this paper was based on ensembles of core-interlayer-shell (CIS) particles, synthesized at Deutsches Kunststoff Institut (DKI), Germany, using a multistage emulsion polymerization process [Ruhl *et al*. (2003); Viel *et al*. (2007)]. As illustrated in Fig. 1, the core-shell particle precursors are approximately 250 nm in diameter and consist of a hard crosslinked polystyrene (PS) core, coated with a thin polymer layer containing Poly methyl methacrylate as a grafting agent, and a soft polyethylacrylate (PEA) outer-shell [Spahn *et al*. (2011)]. In this configuration, the net refractive index contrast between core and shell material is $\Delta n/n \approx 0.11$. The volume fraction of PS core particles in the samples used was about 50% as determined from the initial reaction mix composition, and the material recovered from the reactor had a

rubbery consistency. The material also contained the addition of 0.05 wt. % carbon black which has been found to enhance optical contrast when opalescence occurs [Pursiainen *et al.* (2007)]. A miniextruder (Thermo Scientific, MiniLab) consisting of two counter rotating metallic screws with adjustable speed in the range 1–150 (rpm), and adjustable temperature 25–250 °C was used to compound the material. Typical compounding temperatures were ∼150 °C, and up to 6 g of the opal precursor material was manually fed into the extruder, where a melt was formed and homogenized under the extreme shear conditions provided by the screws. The generated overpressure then forced the material through a narrow-bore stainless steel die, producing rectangular section extrudates of a few mm thickness. At this stage of processing, the polymer sample had a dull green color due to limited particle ordering but was not strongly opalescent.

III. VISCOELASTIC RESPONSE

The viscoelasticity of the polymer opal was studied using an Ares rheometer. This involved applying an oscillatory deformation to the polymer opal sample and measuring the torque response. Two oscillatory rheometric measurements were made, namely, a strain sweep test and a frequency sweep test. The strain sweep test was performed at a fixed angular frequency of 10 rad/s, while the frequency sweep test was performed at a fixed strain amplitude of 0.01. Between 3 and 5 g of the polymer opal sample was heated to 150 °C and pressed into a circular aluminum template to form a polymer opal disk with a diameter of 25 mm and a uniform thickness of 3 mm. The polymer opal disk was subsequently loaded into the test region of a parallel plate flat disc rheometer. Strain sweep and frequency sweep tests were then carried out at 25, 100, and 150 °C to measure the viscoelastic response at the different temperatures. At all the test temperatures, the shell (PEA) material was above its glass transition temperature (-15 °C), and because the PS core was crosslinked, the core structure remained intact. These tests captured the viscoelastic properties of the polymer opal by providing information on the G′ (storage modulus), G″ (loss modulus), and η^* (complex viscosity). Additional steady shearing experiments were attempted, but the material would not deform uniformly at any temperature for large strains within the parallel plate geometry.

The rheological data are shown in Fig. 3 for temperatures of 25, 100, and 125 °C. The 0.01 strain frequency sweeps show that at all temperatures, the material is highly viscoelastic with G′ dominance at all measured frequencies. The values of both G′ and G″ decrease with increasing temperature; however, the G′ dominance at all temperatures is a clear indication of the processing difficulty that this material exhibits. The strain sweeps for the material carried out at 10 rad/s show a very strong strain sensitivity with the linear behavior limited up to an approximate strain level of 0.1. The strain softening shown in Fig. 3 resembles that observed by Kramb and Zukoskia (2011) and Koumakis *et al.* (2008) for a dense suspension of monodisperse spheres and or could be due to a number of factors with slip at the boundary walls a strong possibility. Previous attempts at melt processing this material had met with only partial success [Snoswell *et al.* (2010)], and the rheological data presented here support the view that the material is closer to a rubber than a commercial polymer melt at all test temperatures.

IV. EXPERIMENTAL CONFIGURATION OF MPR TESTING

The MPR was originally designed as a capillary melt processing device [Mackley *et al.* (1995)] and subsequently has been modified to perform a wide range of different
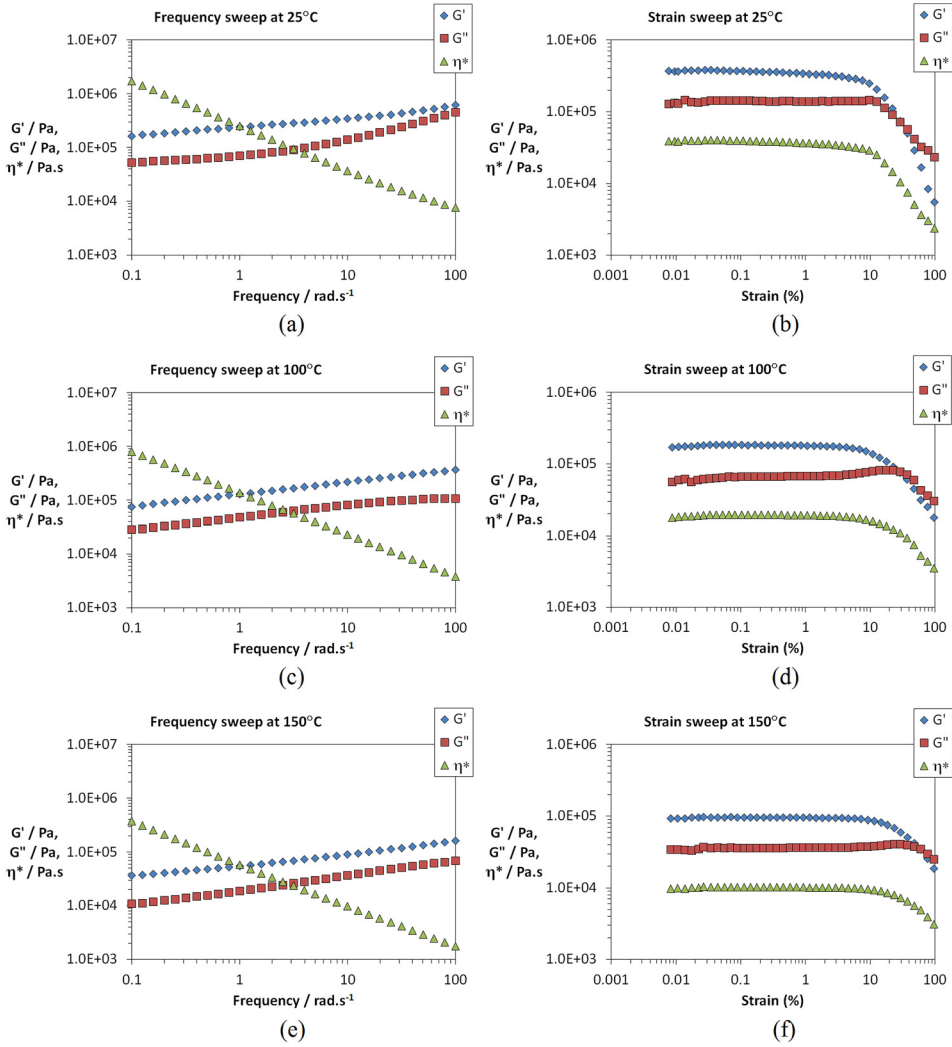
FIG. 3. Linear viscoelastic frequency and strain plots for polymer opal sample: (a) T = 25 °C, strain = 1%, (b) T = 25 °C, frequency = 10 rad/s, (c) T = 100 °C, strain = 1%, (d) T = 100 °C, frequency = 10 rad/s, (e) T = 150 °C, strain = 1%, and (f) T = 150 °C, frequency = 10 rad/s.

rheometric deformations [Mackley and Hassell (2011)]. A further modification was carried out in order to test the deformation behavior of polymer opal samples. In this new configuration, the two servo hydraulic pistons of the MPR were used to deform polymer opal samples in tension, simple shear, and edge shearing. Figures 4(a)–4(c) shows schematically the form of (a) tension, (b) simple shear, and (c) edge shearing applied deformations, and the figure also shows a photograph of the apparatus. Because the opal material was difficult to process, it was necessary to sandwich the material between Polyethylene Terephthalate (PET) tapes. The extruded opal ribbons were positioned between 2 m-long, 4 cm wide PET tapes, and the tapes were then fed under a quartz roller, which had a compressive downward pressure of order 3 bars. The sample was then positioned on a heated glass plate, with the cartridge and plate being preheated to 150 °C. The translation stage was moved horizontally at 1 mm s^{-1} relative to the roller, which
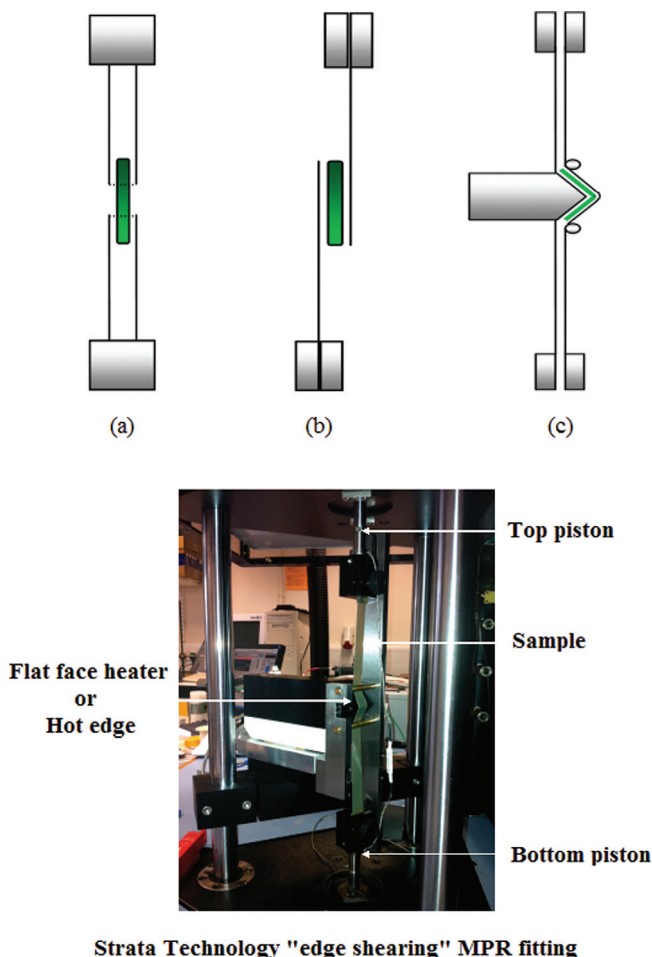
FIG. 4. Schematic diagrams and photograph of MPR. (a) Tensile deformation. (b) Simple shear deformation. (c) Edge shearing deformation geometry and photograph of Strata Technology "edge shearing" attachment.

was free to rotate, pressing the sample into uniform thin films in a squeeze/shear mechanism. The roller was typically set to produce thicknesses of order $100\,\mu$m, and films could be of length from a few centimeters up to several meters. The processing resulted in a certain level of mechanical bonding between the PET tape and opal sample; however, for simple shear and pure extension mechanical tests, there were difficulties.

Samples were prepared in the way indicated in Fig. 4 in order that tensile, simple shear, or edge shearing tests could be carried out. This meant that some of the protective PET tape had to be removed, and this in turn resulted in a test sample that was more difficult to manipulate. Heating of the sample was provided either by bringing a purpose built heated flat face up to the surface of the tape/opal assembly or by using the heated knife edge. This 90° knife edge was mounted on a horizontal traverse that enabled different levels of knife edge penetration to be explored. Three different radii of curvature at the edge of 1, 2, and 5 mm radius were available for testing. Samples were clamped, and by movement of one piston, the samples could be pretensioned. Subsequently, the pistons were then programed to move in a synchronous fashion. Surface temperatures were measured using both an IR thermal probe and a thermocouple.

V. MPR RESULTS AND OPTICAL INTERROGATION

MPR experiments were carried out under different boundary conditions, and samples were subsequently optically interrogated at room temperature in order to establish their photonic response. Figure 5 shows representative photographs of the processed tapes. Figure 5(a) is the starting tape where most of the color contrast comes from the PET outer tapes. Figure 5(b) shows the tape after tensile testing. In this case, the outer PET tapes are only present in the clamped region. A deformation velocity of 0.5 mm/s was applied for a period of 15 s and the central area of the tape was maintained at 100 °C using a flat faced heater block. A weak color change can be seen in Fig. 5(b). Slippage of the sample within the mechanical clamps resulted in only a limited range of strains being able to be achieved, and in addition, the opal material had limited extensibility before mechanical failure.

Difficulties were also experienced with the simple shearing test where, as shown in Fig. 4(b) the sample was gripped with PET sheet on opposite sides. Slip within the clamps and at the opal/PET interface was problematic and levels of deformation again were very limited; however, Fig. 5(c) shows a successfully sheared sample with a deformation velocity of 0.5 mm/s applied for 15 s at 100 °C. The photograph shows some enhanced color contrast and the development of an opalescent appearance. In both the cases of pure extension and simple shear, it was not possible to carry out repeated experiments on the same sample.

The edge shearing, knife edge tests proved to be by far the easiest to perform as the opal sample was protected on each face by the PET tape, and the type of deformation shown schematically in Fig. 4(c) resulted in a compressive load acting between the sample and the tape thereby enhancing adhesion between the two surface. Figure 5(d) shows a representative photograph of a knife edge test where the central region of the tape had been successively oscillated around the knife edge. There are a number of process variables that can be systematically explored, and this photograph was taken with a piston velocity V = 1 mm/s, T = 100 °C, number of oscillations N = 10, and knife edge penetration distance beyond the center line of 8 mm. The initial tensile load on the sample is another variable, but little change was observed over the range of 5–50 N tested. Figure 5(d) shows there is a strong opalescent optical contrast in the region of the processed tape that has passed successively across the knife edge, and this experiment proved to give very reproducible results.
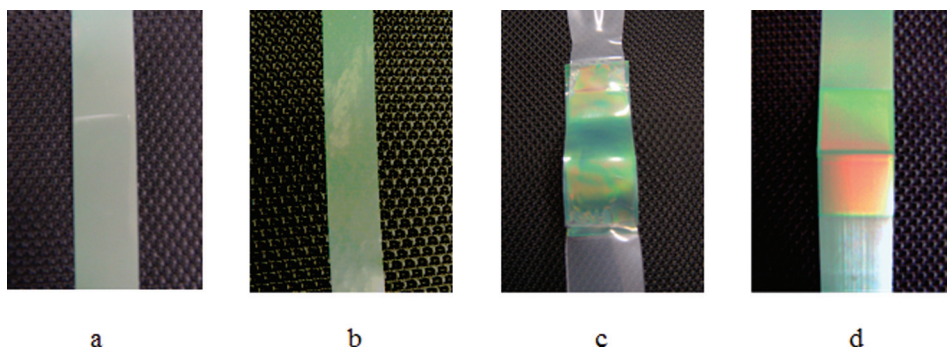

FIG. 5. Representative photographs showing optical appearance of polymer opal samples. (a) Initial tape. (b) Tape after MPR tensile deformation. (c) Tape after MPR simple shear deformation. (d) Tape after successive MPR edge-shearing deformation.

In order to make a more quantitative measure of the optical changes, optical reflectivity spectra was obtained for both faces of the processed opal sample. Measurements were taken using an adapted Olympus BX51 microscope, using a focused spot diameter of about 20 μm, with the light signal collected using suitable focusing optics and a fiber-coupled CCD spectrometer [Finlayson *et al.* (2011b)]. The spectra were normalized using a highly reflective aluminum mirror (bright-field reflectance). Figure 6 shows representative spectra for the tapes photographed in Fig. 5 and from the observed spectra, it is possible to establish more clearly the changes due to the processing.

Figure 6 shows the spectral reflectivity intensity as a function of wavelength for the different samples. The intensity profile as a function of wavelength for the starting material increases with wavelength and shows a mild shoulder. The tensile test sample shows a small change in reflectivity with an enhancement of signal above 600 nm. The simple shear sample shows the beginning of a peak in the region of 600 nm and the knife edge; edge sheared sample shows a clear opalescent peak. Previous modeling of polymer opal spectra as a consequence of progressive crystallization [Snoswell *et al.* (2010)] has linked the peak height with the number of ordered layers within the sample, the peak breadth with the level of ordering, and peak wavelength position with the "Bragg spacing" of the ordered structure. The data show that edge shearing is the most effective of the deformation processes and that tensile deformation alone does not appear to induce ordering that produces opalescence.

When edge shearing experiments were carried out, it was discovered that there were differences in optical properties between the "outer surface" that was furthest away from the knife edge and the "inner" surface which was closest and in Fig. 7; the optical spectra for both the inner and outer surfaces are given for different process conditions. Experiments were carried out as a systematic function of the following variables:

(a)   Temperature T $=$ 25, 50, 100, and 150 °C
(b)   Number of passes N $=$ 1, 10, 100, 200, and 300
(c)   Knife edge penetration X $=$ 6, 8, 10, 12, 14, and 16 mm
(d)   Piston velocity V $=$ 0.1, 0.5, 1, 5, 10, 20, and 30 mm/s.

The complete process conditions for each of the experiments are given in Fig. 7. Additional experiments were carried out at different initial loads, but this was found to
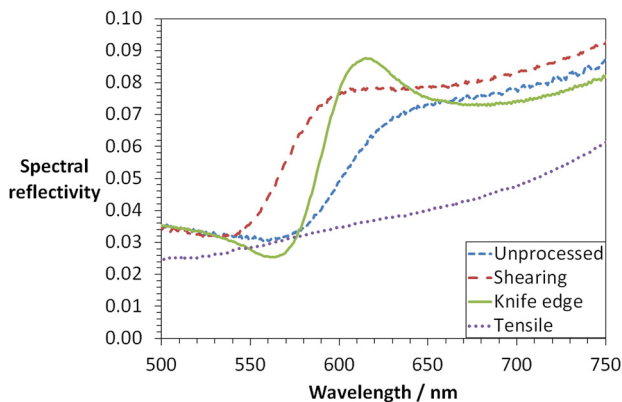
FIG. 6. Representative spectra on the variation of polymer opal outer surface spectral reflectivity as a function of wavelength for different types of deformation applied to the tape for MPR unprocessed tape, MPR simple shear V $=$ 0.5 mm/s, MPR tensile test V $=$ 0.5 mm/s, and MPR edge shearing. MPR processed, V $=$ 1 mm/s. T $=$ 100 °C for all experiments.
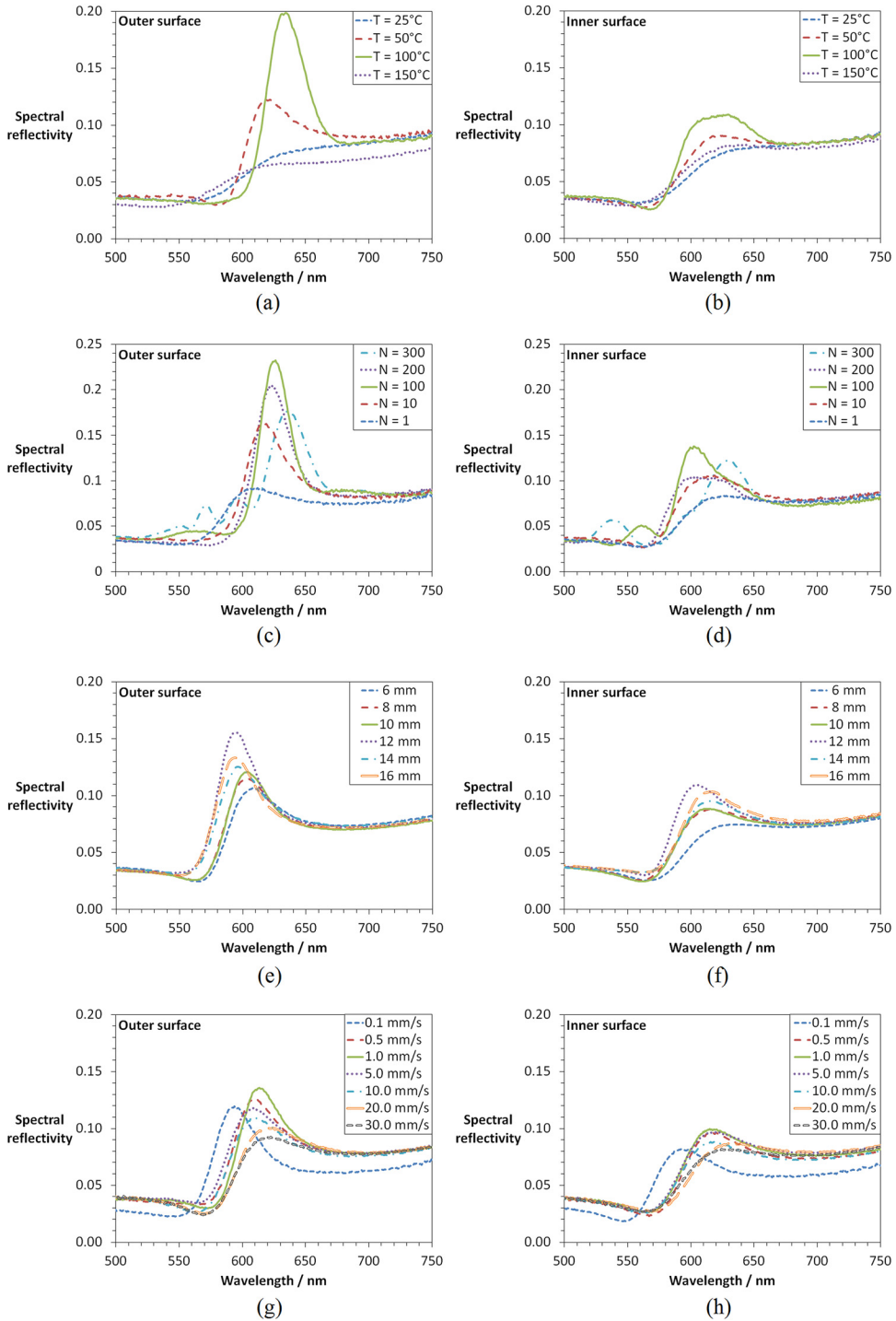
FIG. 7. The effect of processing conditions on the polymer opal spectra: (a) and (b) Temperature, N = 100, V = 1 mm/s, P = 8 mm, L = 5 N. (c) and (d) Number of passes over the knife edge, T = 100 °C, V = 1 mm/s, P = 8 mm, L = 5 N. (e) and (f) Penetration of the knife edge, T = 100 °C, N = 10, V = 1 mm/s, L = 5 N. (g) and (h) Linear velocity of the film, T = 100 °C, P = 8 mm, N = 10, L = 5 N.

have little effect on the results, and all those reported here were carried out at a 5 N initial load. Knife edge curvature was also explored and this again was found to have little effect.

Figures 7(a) and 7(b) show the strong effect that temperature has on the development of opalescence. For all cases considered, the outer surface effects were stronger than the inner surface, although the trends for both surfaces were similar. Both at 25 and 150 °C, there was very little development of opalescence; however, between these two temperatures, there was a strong effect, with 100 °C experiment showing the largest opalescent peak. Whilst it was not necessarily surprising that an opalescent peak did not develop at 25 °C, it was surprising that there was no opalescence at 150 °C. Higher temperatures do promote thermal motion, and so it is possible that shear-ordered crystalline regions are dissolved at the higher temperatures once shearing has ceased. The corresponding rheology changes as a function of temperature that were shown in Fig. 3 did not indicate any significant change in rheological profile other than a general reduction in modulus with temperature suggesting that the change in opalescence could not be directly detected by a rheology change.

The number of passes also had a significant effect on the observed level of opalescence, and this is shown in Figs. 7(c) and 7(d). One pass produces a small effect, and maximum peak height is achieved at 100 passes. After that, the peak height signal decreases with a further 200 and 300 passes. Again the results are surprising with a clear maximum developing followed by an unexpected decrease. Colloidal crystallization is known to be strongly induced by wall effects [see, for example, van Blaaderen *et al.* (1997)], and in the polymer opal case, surface growth is believed to develop from the surface into the interior of the sample with each shear pass. A possible explanation of the decrease from the maximum may be that the crystallized phase of the opals is stationary with respect to the outer foils, and it is only the disordered inner part of the phase that flows. As crystal planes develop, growing in from the wall, the ratio of ordered stationary phase and disordered "flowing" phase changes. This in effect increases the local shear at the boundary between the disordered and ordered phases throughout crystal growth, despite the fact the bulk shear conditions are constant. When the stationary crystal phase occupies a large proportion of the sample thickness, local shear at the growing crystal boundary becomes very large and starts to break up multiple crystal layers causing degradation of the color.

Figures 7(e) and 7(f) show the effect of knife edge penetration, and once again a maximum was detected within the experimental range. As knife edge penetration increased from 6 to 12 mm, the opalescent peak height increased. Then for penetration of 14 and 16 mm, there was a progressive decrease. Conceptually, a disordered arrangement of spheres requires individual sphere to move by up to 0.5 of its diameter relative to its neighbor to find a location in an ordered lattice. Therefore, it might be expected for shear strain magnitudes of 0.5 to be optimal for crystallization. Since shear magnitude is controlled by knife edge penetration, this may account for the optimum positions observed.

Finally, the effect of piston velocity is shown in Figs. 7(g) and 7(h). These graphs too show a peak effect at 1 mm/s with a progressive increase and then decrease in peak height with increasing piston velocity. The effect of velocity can be interpreted as changing the shear rate. This impacts on the ordering process by changing the proportion of viscous and elastic deformation during shear, with only viscous shear producing sphere-sphere movement and alignment into the ordered crystal state.

For any set of process conditions, the results were essentially reproducible; when repeated and taken as a whole, the data show a complex, but reproducible sensitivity to the process variables tested. This in turn suggests that the mechanisms controlling the development of ordering is also complex and not directly related to the materials rheology, which, for example, showed a weak but monotonic effect to temperature.

(a) (b) (c)
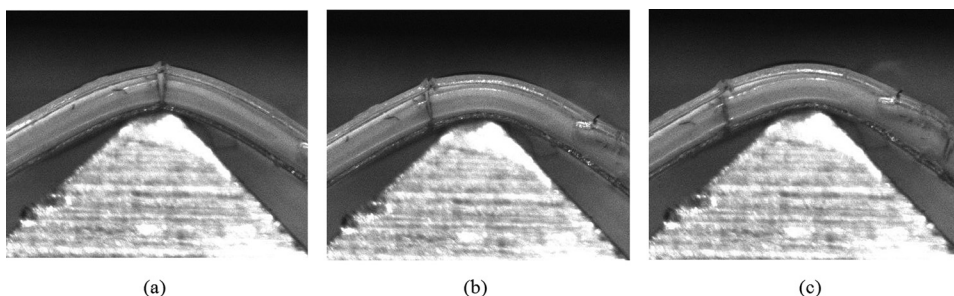
FIG. 8. Side view photographic sequence of polymer opal sample being edge sheared from right to left. (a)–(c) T = 25 °C. Piston tape translation velocity = 1 mm/s. Approximate thickness of sample = 0.5 mm. The photograph shows the V metal edge and the foam, sandwiched between a top and bottom PET tape. The vertical marker line shown in 7(a) is seen to shear as the sample progressively moves from right to left over the edge as shown in Figs. 7(b) and 7(c).

VI. DEFORMATION OF MODEL MATERIAL

The edge shearing, knife edge deformation of the polymer opal sample sandwiched between plastic sheets is both an unusual and a complicated deformation and so in an attempt to help understand the type of deformation that had occurred, a model deformation was carried out using a thicker foamed material.

An initial 3 mm thick polyethylene foam strip was fixed with double sided adhesive tape to the PET tape. The assembly was then in turn fixed to the pistons of the MPR in the edge shearing mode and then tensioned. It was possible to draw lines on the edge of the compressed foamed material as shown in the photographs of Fig. 8 and from this determine the strain deformation experienced during the edge shearing experiment. From photographs of the type shown in Fig. 8, it can be seen that the deformation is dominantly simple shear as initially conjectured by Finlayson *et al.* (2011b) and the maximum level of shear strain achieved for the compressed foam sample was of order 0.5. The results indicate that the model knife-edge shearing was predominantly simple shear, and it is possible that this is also true for the opal sample which unfortunately could not be tested in this way because the thickness of the sample was too thin and side view optical observation was not possible. Because the geometry of the model system is similar for the opal samples, we believe the dominant type and level of shear strain is similar in both cases, and this would correspond for the opal tests to an approximate applied shear rate of $0.05 \, \text{s}^{-1}$ at the lowest piston speed and $15 \, \text{s}^{-1}$ at the highest piston speed.

VII. DISCUSSION AND CONCLUSIONS

The linear viscoelastic rheology of the tested polymer opal samples had rubbery like properties, and the material was on the edge of processability. Both aspects result in a rheologically complex material with a high level of elasticity. Normally, the polystyrene colloidal particles in the solvent-free core shell material would be expected to be disordered; however, shear induced ordering occurs under certain processing conditions.

The ordering of colloidal suspensions in low viscosity matrix fluids has been reported before [see, for example, Liu *et al.* (1993)]; however, the transition, even in this relatively simple fluid, from low shear disorder to intermediate shear order and then potentially high shear disorder has not been extensively studied, mapped, or modeled. In the case of polymer opals the situation is even more complex. The high level of elasticity as reported in this paper resulted in material that was both strain and strain rate dependent. The

structure of the solvent-free rubbery material is also complex as the mobile shell phase of the material is grafted to the core particle. The MPR experimental results indicate that simple tension did not induce ordering within the material; however, the direct application of a single pass simple shear did induce some ordering. Both these experiments suffered from experiment difficulties, and so only very limited experiments were possible Multiple edge shearing around a knife edge did induce significant ordering. As with low viscosity matrix suspensions [see, for example, Vermant and Solomom (2005)], the application of repeated simple shear oscillations enhances ordering kinetics.

Successive edge shearing proved to be the only effective experimental way of inducing ordering, and this was investigated as a function of a number of process variables. When each process variable was scanned, an optimum range for opal formation was discovered, namely, a process temperature of 100 °C, 100 oscillations, a knife edge penetration of 12 mm, and a piston velocity of 1 mm/s. In addition, the outer surface of the opal sample always showed a stronger opalescence to the inner surface. These results indicate that ordering kinetics are influenced by a complex series of variables with nucleation and growth of ordering being controlled by many different factors.

The MPR model edge shearing experiments demonstrated that the main deformation for edge shearing was simple shear; however, the difference in opalescence for the polymer opal sample between the outer and inner surfaces suggest that the opal deformation is more complex than the model deformation. The polymer opal edge shear deformation will have additional factors including compressive squeeze flow deformation and almost certainly wall slip between the PET and Opal interfaces. The fact that the opalescence on the top and bottom faces was different for any one set of experiments also highlights potential differences between the apparently homogeneous simple shear deformation of the model experiments and a more complex deformation for the opal sample.

Clearly many uncertainties remain in relation to both the Polymer Opal material and the fact that the unusual edge shearing around a knife edge can be so effective at inducing opalescent ordering of particles. There is therefore a need for further experiments, and in particular, there is scope for a rich vein of modeling that can help to understand the deformation, rheology, ordering, and resulting opalescence of this remarkable material.

ACKNOWLEDGMENTS

References

Ackerson, B. J., "Shear induced order and shear processing of model hard sphere suspensions," J. Rheol. **34**(4) 553 (1990).

Ackerson, B. J., and P. N. Pusey, "Shear-induced order in suspensions of hard spheres," Phys. Rev. Lett. **61**(8), 1033–1036 (1988).

Alfrey, T., E. B. Bradford, J. W. Vanderhoff, and G. Oyster, "Optical properties of uniform particle-size latexes," J. Opt. Soc. Am. **44**, 603–607 (1954).

Catherall, A. A., J. R. Melrose, and R. C. Ball, "Shear thickening and order–disorder effects in concentrated colloids at high shear rates," J. Rheol. **44**(1), 1–25 (2000).

Chen, L. B., C. F. Zukoski, B. J. Ackerson, H. J. M. Hanley, G. C. Straty, J. Barker, and C. J. Glinka, "Structural changes and orientational order in a sheared colloidal suspension," Phys. Rev. Lett. **69**(4), 688–703 (1992).

Dealy, J. M., and J. Wang, *Melt Rheology and Its Applications in the Plastics Industry* (Springer, Munich, 2013).

Finlayson, C. E., C. Goddard, E. Papachristodoulou, D. R. E. Snoswell, A. Kontogeorgos, P. Spahn, G. P. Hellmann, O. Hess, and J. J. Baumberg, "Ordering in stretch tunable polymeric opal fibers," Opt. Express **19**, 3144–3154 (2011a).

Finlayson, C. E., and J. J. Baumberg, "Polymer opals as novel photonic materials," Polym. Int. **62**(10), 1403–1407 (2013).

Finlayson, C. E., P. Spahn, D. R. E. Snoswell, G. Yates, A. Kontogeorgos, A. I. Haines, G. P. Hellmann, and J. J. Baumberg, "3D bulk ordering in macroscopic solid opaline films by edge-induced rotational shearing," Adv. Mater. **23**, 1540–1544 (2011b).

Hachisu, S., Y. Kobayashi, and A. D. Kose, "Phase separation in monodisperse latexes," J. Colloid Interface Sci. **42**(2), 342 (1973).

Haw, M. D., W. C. K. Poon, and P. N. Pusey, "Direct observation of oscillatory-shear-induced order in colloidal suspensions," Phys. Rev. E **57**(6), 6859–6864 (1998).

Koumakis, N., A. B. Schofield, and G. Petekidis, "Effects of shear induced crystallization on the rheology and ageing of hard sphere glasses," Soft Matter **4**, 2008–2018 (2008).

Kramb, R. C., and C. F. Zukoskia, "Nonlinear rheology and yielding in dense suspensions of hard anisotropic colloids," J. Rheol. **55**(5), 1069–1084 (2011).

Liu, A. J., and S. R. Nagel, "Granular and jammed materials," Soft Matter **6**, 2869–2870 (2010).

Liu, J., D. A. Weitz, and B. J. Ackerson, "Coherent crystallography of shear-aligned crystals of hard-sphere colloids," Phys. Rev. E **48**(2), 1106–1114 (1993).

Mackley, M. R., and D. G. Hassell, "The multipass rheometer: A review," J. Non-Newtonian Fluid Mech. **166**(9-10), 421–456 (2011).

Mackley, M. R., R. T. J. Marshall, and J. B. A. F. Smeulders, "The multipass rheometer," J. Rheol. **39**(6), 1293–1309 (1995).

McMullan, J. M., and N. J. Wagner, "Directed self-assembly of suspensions by large amplitude oscillatory shear flow," J. Rheol. **53**(3), 575–588 (2009).

Mewis, J., W. J. Frith, T. A. Strivens, and W. B. Russel, "The rheology of suspensions containing polymerically stabilized particles," AIChE J. **35**(3), 415–422 (1989).

Pursiainen, O. L. J., J. J. Baumberg, H. Winkler, B. Viel, P. Spahn, and T. Ruhl, "Nanoparticle-tuned structural color from polymer opals," Opt. Express **15**(15), 9552–9561 (2007).

Pursiainen, O. L. J., J. J. Baumberg, H. Winkler, B. Viel, and T. Ruhl, "Compact strain-sensitive flexible photonic crystals for sensors," Appl. Phys. Lett. **87**(10), 1902–1905 (2005).

Ruhl, T., P. Spahn, and G. P. Hellmann, "Artificial opals prepared by melt compression," Polymer **44**, 7625–7634 (2003).

Ruhl, T., P. Spahn, H. Winkler, and G. P. Hellmann, "Large area monodomain order in colloidal crystals," Macromol. Chem. Phys. **205**, 1385–1393 (2004).

Snoswell, D. R. E., A. Kontogeorgos, J. J. Baumberg, T. D. Lord M. R. Mackley, P. Spahn, and G. P. Hellmann, "Shear ordering in polymer photonic crystals," Phys. Rev. E **81**, 020401 (2010).

Spahn, P., C. E. Finlayson, W. Mbi Etah, D. R. E. Snoswell, J. J. Baumberg, and G. P. Hellmann, "Modification of the refractive-index contrast in polymer opal films," J. Mater. Chem. **21**, 8893–8897 (2011).

Sussman, J., D. R. E. Snoswell, A. Kontogeorgos, J. J. Baumberg, and P. Spahn, "Thermochromic polymer opals," Appl. Phys. Lett. **95**(17), 173116 (2009).

Trappe, V., V. Prasad, L. Cipelletti, P. N. Segre, and D. A. Weitz, "Jamming phase diagram for attractive particles," Nature **411**(14), 772–775 (2001).

van Blaaderen, A., R. Ruel, and P. Wiltzius, "Template directed colloidal crystallisation," Nature **385**, 321–324 (1997).

Vermant, J., and M. J. Solomon, "Flow-induced structure in colloidal suspensions," J. Phys.: Condens. Matter **17**, 187–216 (2005).

Viel, B., T. Ruhl, and G. P. Hellmann, "Reversible deformation of opal elastomer," Chem. Mater. **19**, 5673–5679 (2007).

White, J. L., and K. J. Kim, *Thermoplastic and Rubber Compounds: Technology and Physical Chemistry* (Hanser, Munich, 2007–2008).